



### **Science Arts & Métiers (SAM)**

is an open access repository that collects the work of Arts et Métiers Institute of Technology researchers and makes it freely available over the web where possible.

This is an author-deposited version published in: <https://sam.ensam.eu>  
Handle ID: <http://hdl.handle.net/10985/6752>

#### **To cite this version :**

Bassel ASLAN, Julien KORECKI, Thimoté VIGIER, Eric SEMAIL - Influence of Rotor Structure and Number of Phases on Torque and Flux Weakening Characteristics of V-Shape Interior PM Electrical Machine - Journal of Energy and Power Engineering p.1461-1471 - 2012

Any correspondence concerning this service should be sent to the repository

Administrator : [scienceouverte@ensam.eu](mailto:scienceouverte@ensam.eu)



# Influence of Rotor Structure and Number of Phases on Torque and Flux Weakening Characteristics of V-shape Interior PM Electrical Machine

Bassel Aslan, Julien Korecki, Thimoté Vigier and Eric Semail

*Arts et Metiers PARISTECH, L2EP Laboratory, 59046 Lille, France*

Received: September 09, 2011 / Accepted: December 13, 2011 / Published: September 30, 2012.

**Abstract:** This paper investigates the influence of the rotor structure on torque and flux weakening region of V-shape IPM (interior permanent magnet) machine from TOYOTA PRIUS type, more specifically, keeping always the same magnet volume, the effect of the open angle between the two magnet segments of each V-shape pole on the machine performance is studied. Moreover, in order to examine the impact of phase number on the machine characteristics, PRIUS structure is transformed into 5-phase machine of the same type and dimensions. As well, an optimization procedure is carried out to determine the optimal open angle according to main characteristics. The previous investigation is done by using a free FEM (finite elements methods) program coupled with another optimization program. Using this obtained methodology the study analyzes for 3-phase and 5-phase machine the average and pulsation of torque, cogging torque, phase Electro-Motive Force EMF, constant power operating capability.

**Key words:** V-shape magnet machine, straight-shape magnet machine, multi-phase machine, torque ripples, flux weakening.

## 1. Introduction

Permanent magnet motor (PM) is one of the most attractive motors applied in compact electric propulsion system, due to its high efficiency, high reliability, and power density. The interior permanent magnet motor (IPM) adds a reluctant torque generated by rotor saliency to the original magnetic torque. Therefore, this motor has higher torque density compared with surface mounted permanent magnet motors (SMPM). Also extended flux weakening region is one of the advantages of IPM motors, because of their reluctance effect and rigid rotor structure which permits to reach high speed [1]

On the other hand, the major drawback of IPM structure is high torque ripple because of the

non-sinusoidal magnetic field distribution in the air gap, which implies harmonic components of the EMF, leading to torque ripple even in the case of sinusoidal current supply. As well, cogging and reluctance torque are other important sources of torque oscillation. The shape and configuration of permanent magnets in the rotor is an essential factor to consider during IPM design, trying to create an optimum spatial flux linkage.

Nonlinear finite element program “femm” is used to study and optimize one of the rotor magnet configurations in V-shape electrical machine. The considered magnet configuration is the open angle of V-shape pole. The angle is optimized according to the machine general performances (average torque, torque ripple, flux weakening region). Later on in this paper the pole open angle  $\alpha$  will be replaced by the value of  $h$  (the distance between the middle point of each magnet pole and the outer circumference of the rotor) (see Fig. 1). This paper studies two machines which have the same type and dimensions of TOYOTA PRIUS machine [2],

---

**Corresponding author:** Eric Semail, professor, research fields: multiphase drives, fault tolerant systems; E-mail: eric.semail@ensam.eu

but they differ in the phase number (3 and 5). Comparisons are done to find out the optimum pole open angle in both machines, hoping to benefit from the advantages of 5-phase machine over the classic 3-phase structure: better fault tolerance, lower pulsating torque, splitting the power across more inverter legs, and lastly additional degrees of freedom can be used for different purposes [3]. In order to have a fair comparison, the total volume of permanent magnets is kept constant in both machines.

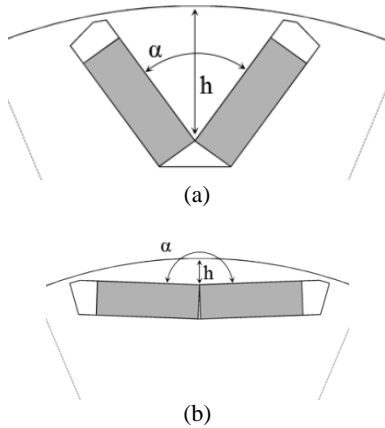


**Fig. 1** Permanent magnet configurations between (a)  $h_{max}$  and (b)  $h_{min}$

## 2. Three-Phase TOYOTA PRIUS Type Machine

A 3-phase, 8 poles, 48 slots IPM motor is considered in this study. This motor has a distribution winding with  $q = 2$  (number of slots per pole and per phase). The motor has the same structure and dimensions as the machine Prius THS II 2004 [2]. The rotor configuration is also the same type of V-shape magnets, but with different pole open angle. This paragraph studies and compares the variation of the machine performance with this angle ( $h$  value), including the original PRIUS value ( $h = 10.96$  mm), **Fig. 2** presents a cross section of this machine.

The motor is supplied with three sinusoidal shifted currents of amplitude 212 A. Average torque is the first to be studied, and different sources of torque oscillation are examined (cogging and reluctant torque), then

torque-speed characteristic is determined (flux weakening region).

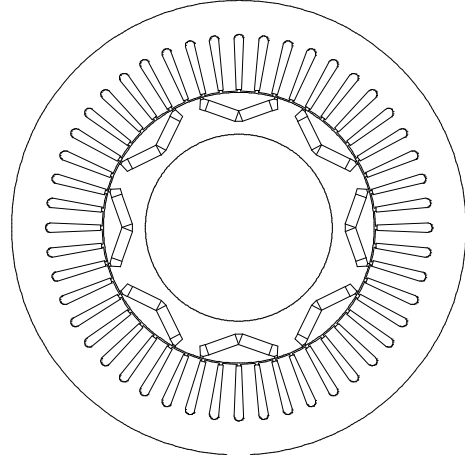


**Fig. 2** Cross section in 3-phase TOYOTA PRIUS type machine.

### 2.1 The Average Torque $T_{average}$

Instead of searching the static torque [4], this paper uses FEM program “femm” to calculate the average torque of the machine according to the electrical angle  $\psi_e$  (phase difference between current and EMF), considering different values of the pole open angle, always without changing the volume neither the shape of magnets.

**Fig. 3** shows the curves of average torques which correspond to different  $h$  values. It can be noted that curves of average torque do not vary so much with the value of  $h$  (magnet open angle). However, it appears that PRIUS structure with  $h = 10.96$  mm produces the highest torque among all the other configurations at  $\psi_e = -45^\circ$ . This is due to the added reluctant torque which is likely more affected by the value of  $h$  than the electromagnetic one, simply because changing the magnet open angle  $h$  affects the paths of flux paths resulting in inductance variation ( $L_d, L_q$ ).

**Fig. 4** shows the no-load EMF frequency spectrums for 10 different values of  $h$ , as it can be noted, no big difference in the amplitude of the first harmonic between examined configurations, which proves that pole open angle does not have remarkable effects on the average electromagnetic torque.

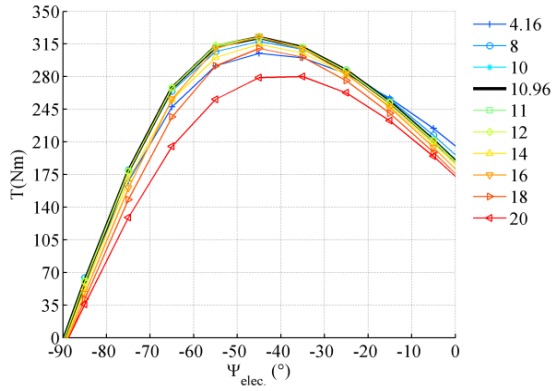


Fig. 3 Average torque versus electrical shift angle.

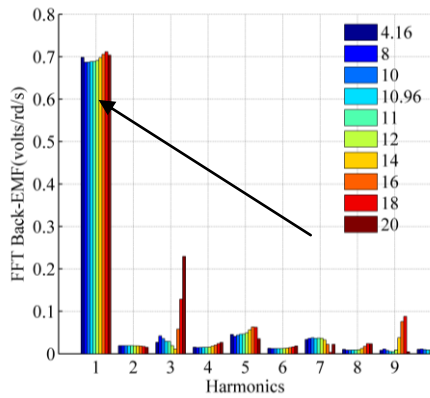


Fig. 4 No load EMF frequency spectrums for  $h = [4.16\text{mm}; 20\text{mm}]$ .

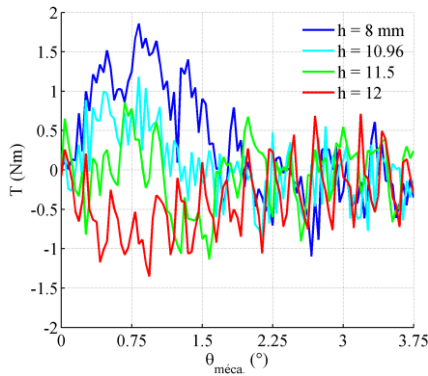


Fig. 5 Cogging torque for 3-phase PRIUS type machine.

### 2.2 The Cogging Torque

Torque oscillation is one of the important characteristic in traction application; therefore, this paper investigates the effect of magnet open angle on the torque ripple. First of all, the cogging torque sensibility to  $h$  is studied using a methodology consisting in a coupling between an optimization

program in Matlab and the FEM “femm”. This methodology helps to find the optimal magnet open angle  $h_{\text{optimum}}$  which generates the minimum cogging torque [5]. The chosen criteria for this optimization is minimizing the RMS value of cogging torque, and the result is  $h_{\text{optimum}} = 11.51$  mm, while value of  $h$  in original PRIUS machine is  $h = 10.96$  mm. Fig. 5 shows the cogging torque for different magnet open angles.

### 2.3 Torque Ripples

To continue with torque oscillation phenomena, this paper studies the effect of pole open angle on the torque ripple while the machine is operating with different electrical angle  $\psi_e$ . In order to have comparable values, relative amplitude of oscillation is considered  $\Delta T/T_{\text{average}}(\psi_e, h)$ .

Fig. 6 shows the curves of relative torque oscillation, where each curve represents the torque oscillation of one configuration ( $h$ ) according to the electrical angle  $\psi_e$ . By observing the curves close to  $\psi_e = 0$ , it can be noticed that the configuration with  $h = 18$  mm has the lowest relative oscillation in torque (down to 8%). This result corresponds to the EMF frequency spectrums (Fig. 4) where the seventh harmonic which can disturb the torque (with the fifth one) is almost null in this configuration ( $h = 18$  mm).

Nevertheless, as the motor must work in a wide range of torque, it can be considered that a more global comparison is necessary. So the average value of torque relative oscillation is calculated along the flux weakening region  $\psi_e \in [-80^\circ, -45^\circ]$ . Fig. 7 presents this average according to  $h$ , where it can be noted that the structure with  $h = 8$  mm has the lowest average of torque relative oscillation (about 19%) all over the flux weakening region starting from maximum torque point at base speed (1200 rpm) up to the maximum speed of 7000 rpm (corresponding to  $\psi_e$  close to  $-80^\circ$ ).

## Influence of Rotor Structure and Number of Phases on Torque and Flux Weakening Characteristics of V-shape Interior PM Electrical Machine

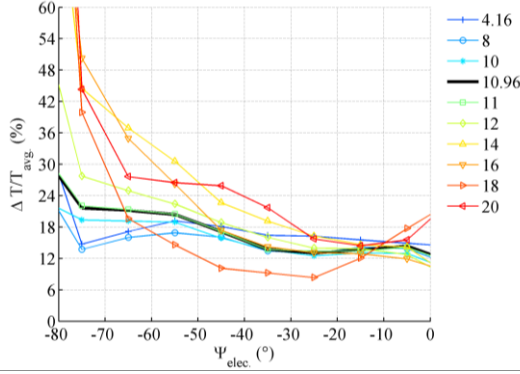


**Fig. 6** Torque ripple in 3-phase PRIUS type machine ( $I_p = 212$  A).

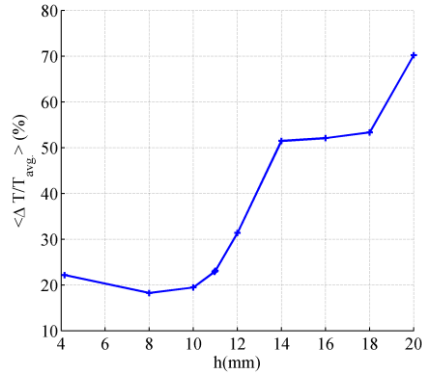


**Fig. 7** The average of relative torque ripples over the flux weakening region.

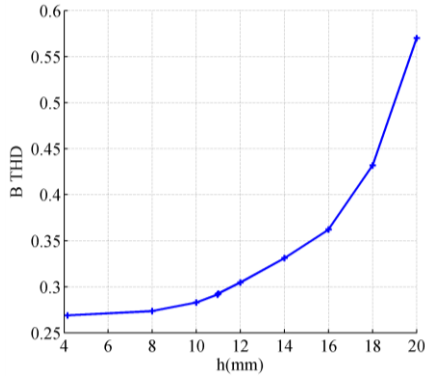


**Fig. 8** THD of magnetic flux density in the air gap.

### 2.4 Magnetic Flux Density in the Air Gap

In this study also the THD (total harmonic distortion) of magnetic flux density is calculated for different configurations as an alternative index of the iron loss reduction. The optimum  $h$  which minimizes the THD of the flux density distribution in the air gap is searched [6]. Fig. 8 shows the THD value for different

pole open angle, and simply it can be noticed that straight-shape magnets structure with  $h = 4.16$  mm has the lowest THD value.

### 2.5 Flux Weakening Region

Power-speed and torque-speed characteristics and how flux weakening region is affected by the magnet open angle ( $h$ ) are another important performances of the machine. First of all,  $L_d$ ,  $L_q$  are calculated using

FEM software and in order to consider iron saturation this calculation is done for three different load currents (amplitude 212 A, 150 A, 99 A).

Figs. 9a and 9b present the calculated values of  $L_d$ ,  $L_q$  according to the magnet open angle. The value ( $L_q - L_d$ ) which decides the amount of added reluctant torque is also represented in Fig. 9c. The functionality region of the machine is limited by two main factors, maximum current due to thermal and magnetic constraints and maximum voltage imposed by the DC bus of the inverter [7]

$$\begin{aligned} i_d^2 + i_q^2 &\leq I_{\max}^2 \\ v_d^2 + v_q^2 &\leq V_{\max}^2 \Rightarrow \\ (R_s i_d - p\Omega L_q i_q)^2 + \\ (R_s i_q + p\Omega(\Phi_f + L_d i_d))^2 &\leq V_{\max}^2 \end{aligned} \quad (1)$$

As it can be seen in the last two inequalities, the phase resistance  $R_s$ , permanent magnet flux  $\Phi_f$ , and the two inductances  $L_d$ ,  $L_q$  can directly define the flux weakening capability and possible speed range.

The electromagnetic torque can be written as:

$$T = \frac{3p}{2} (i_q \Phi_f + i_d i_q (L_d - L_q)) \quad (2)$$

Of course the last calculation does not consider the inductance variation because of saturation, neither the iron loss in the machine. The machine PRIUS second generation THS II 2004 is supplied by an inverter working on 500 V DC bus, and giving a maximum current amplitude of 230 A [4]. Considering those limits with the calculated parameters, and by applying a flux weakening strategy the curves torque-speed, and power-speed of the machine can be drawn. Fig. 10

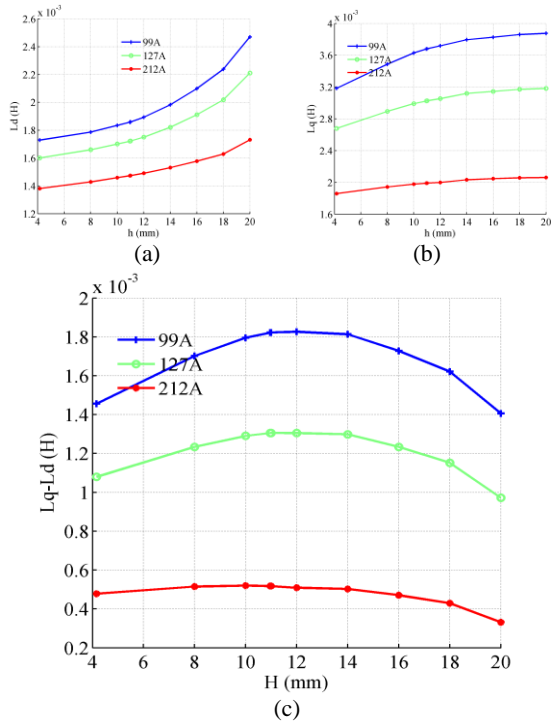


Fig. 9 (a)  $L_d$ , (b)  $L_q$  and (c)  $L_q - L_d$  calculated for 3-phase PRIUS type machine.

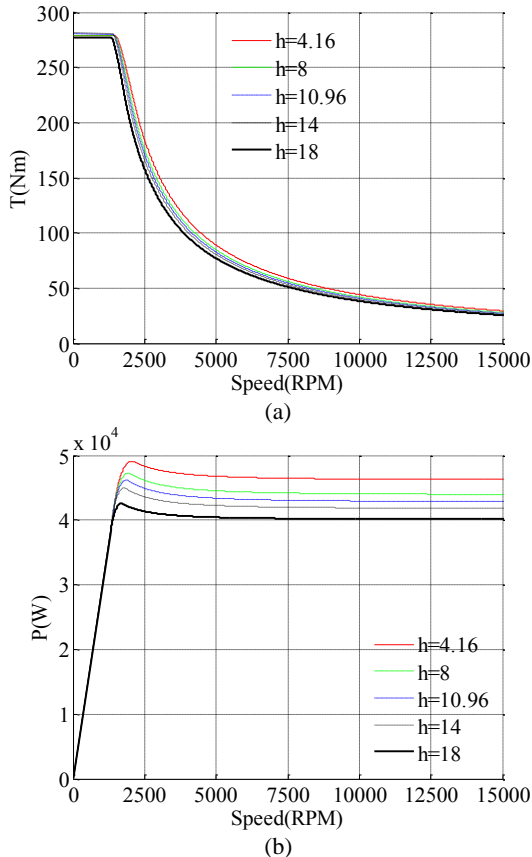


Fig. 10 (a) Torque-speed, (b) power-speed characteristics for the 3-phase PRIUS type machine for  $I_p = 212$  A

shows the curves which present the torque/power-speed characteristics of the machine for 5 magnet configuration (5 values of  $h$ ). Those curves are calculated depending on a strategy of flux weakening which minimizes the Joule losses at base speed, and then for each higher rotating speed it forces the machine to function with the maximum possible torque. Furthermore, this strategy considers the reluctant torque while choosing the optimum point of functionality. It can be noted from Fig. 10 (power-speed) that all structures have a constant power operating capability, while the machine with straight-shape magnets ( $h = 4.16$  mm) has the best characteristics along the flux weakening region, due to the highest torque produced by this configuration up to reach high speeds. However, the configurations PRIUS ( $h = 10.96$  mm) and ( $h = 14$  mm) are the best at basic speed region ( $L_q - L_d$ ) where they produce higher torque than the other structures.

In fact this result corresponds to the inductances calculations ( $L_d$ ,  $L_q$ ) in Fig. 9 which shows that the structures close to PRIUS machine ( $h$  is close to 11 mm) benefit more from the reluctant effect than the others, owing to their higher value  $L_q - L_d$ .

Nevertheless, this difference in reluctance is clearer for lower currents, as it can be noticed in Fig. 9 for a lower current of 99 A.

When low current is applied the reluctance indication  $L_q - L_d$  varies much more with  $h$  than in the case of higher currents, and that because the machine with lower currents is less saturated, and consequently the role of magnet structure (pole open angle) becomes more important.

Fig. 11 shows the torque-speed characteristics of the machine for the same five values of  $h$  but with lower current amplitude of 127 A. Here the structure with ( $h = 14$  mm) can be easily classified as the best choice at low speed application (more generated torque), while the straight-shape magnets structure stays the best choice for higher speeds along the flux weakening

region owing to its high ratio: magnet flux/ $L_d$ . The author in

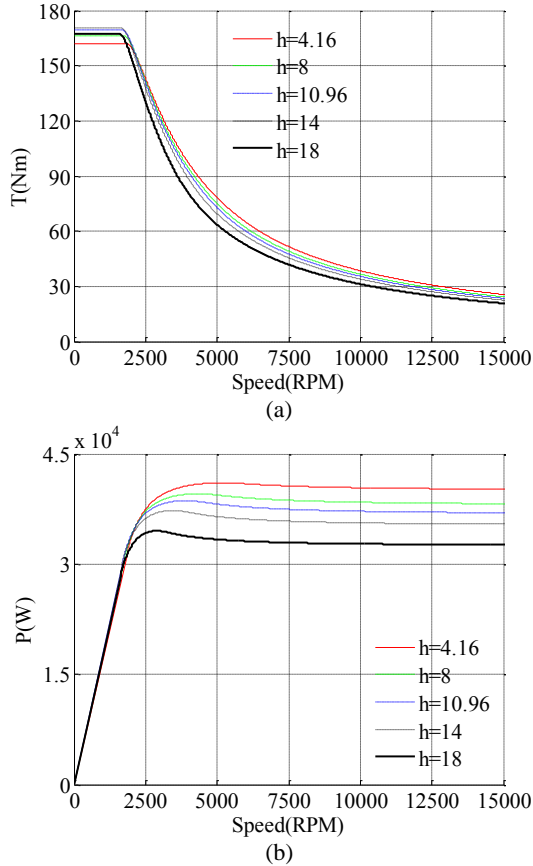


**Fig. 11 (a) Torque-speed; (b) power-speed characteristics for the 3-phase PRIUS type machine for  $I_p = 127$  A.**

Ref. [8] finds similar results but with fractional slot winding machine.

In this study the magnet volume is kept always constant, but it worth to mention that V-shape magnets allow installing bigger magnet segments which give more torque at low speed thanks to higher linkage, but in the same time bigger magnets lead to shorter flux weakening region due to the decrease in d-axis inductance [9].

### 3. Five-Phase TOYOTA PRIUS Machine Type

The idea behind the comparison between PRIUS machine and a 5-phase machine is to examine the effects of the phase number on its performance, while keeping as possible as the same rotor structure, dimensions, and winding type (integral slot winding).

Therefore, a little modification is done to allow PRIUS type machine to support 5-phase integral slot winding by reducing the slots number from 48 to 40, then as a result a winding of one slot per pole and per phase ( $q = 1$ ) is gotten. Fig. 12 presents a cross section of this machine. The motor is supplied with five sinusoidal shifted currents of amplitude 127 A keeping the same linear current density as in the original PRIUS machine.

Like in the last paragraph, this one studies and compares the variation of the machine performance with the pole open angle ( $h$  value). The average torque is the first to be studied considering other degrees of freedom offered by this multiphase machine (other EMF harmonics. Besides that, different sources of torque oscillation are examined (cogging torque, torque ripple), then torque-speed characteristic is determined (flux weakening region).

#### 3.1 Average EMF – Torque $T$ (Considering the main EMF harmonic)

First of all the average torque of the machine supplied with five sinusoidal shifted currents is calculated using FEM program “femm”. Fig. 13 shows the curves of average torques which correspond to different  $h$  values. No big difference can be noted between this 5-phase machine and 3-phase PRIUS one. The curves of average torque do not vary so much with the value of  $h$ . However, it appears that the machine with  $h = 10.96$  mm (PRIUS structure) produces also the highest torque among all the other configurations at  $\psi_e = -45^\circ$ .

Fig. 14 shows the no-load EMF frequency spectrums for ten different values of  $h$ , where it can be seen that PRIUS structure ( $h = 10.96$  mm) has a low main harmonic amplitude. This means that if the maximum average torque is obtained by PRIUS configuration in Fig. 13 it is due to its reluctant torque.

Of course with this new winding, much more harmonic of electromotive force can be noticed.

However, it will be seen in next paragraph that these harmonics does not produce more torque pulsations in the 5-phase configuration.

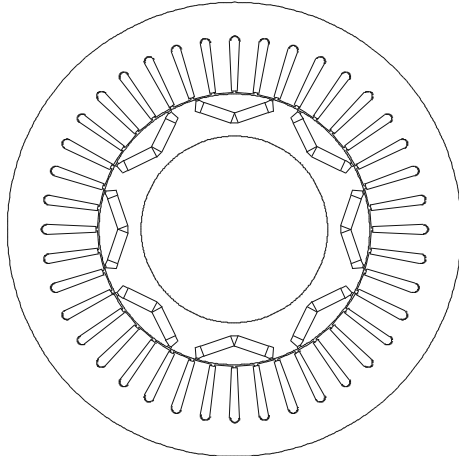


Fig. 12 Cross section in 5-phase PRIUS type machine.

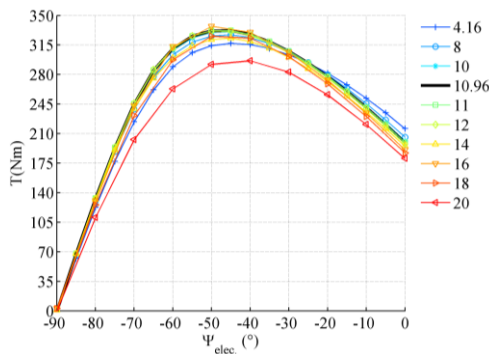


Fig. 13 Average torque for 5-phase PRIUS type machine.

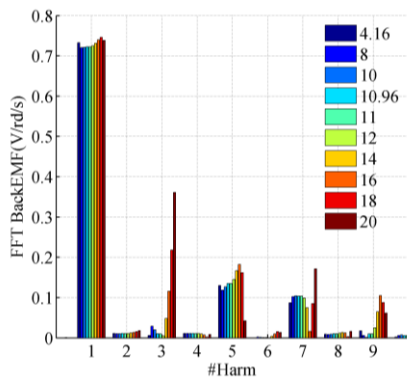


Fig. 14 No load EMF frequency spectrums for  $h = [4.16 \text{ mm}, 20 \text{ mm}]$ .

### 3.2 Benefit of Third EMF Harmonic absence for Lower Peak Current

A 5-phase machine can be divided into 2 two-phase fictitious machines which are mechanically coupled

but magnetically independent. Moreover, each fictitious machine is characterized by a family of particular EMF harmonics, therefore, the main fictitious machine is sensitive to the first current harmonic, while the other one (secondary machine) interacts mainly with the third current harmonic [10]. In a 5-phase machine the third, fifth and seven harmonics of EMF do not interact with the first harmonic of current.

Furthermore by observing the frequency spectrums of the EMF in Fig. 14, the torque generated by each fictitious machine for all configurations can be decided. For example the configuration corresponds to  $h = 12 \text{ mm}$  has no EMF third harmonic, consequently, whatever is the input current the average torque generated by the secondary fictitious machine will be null.

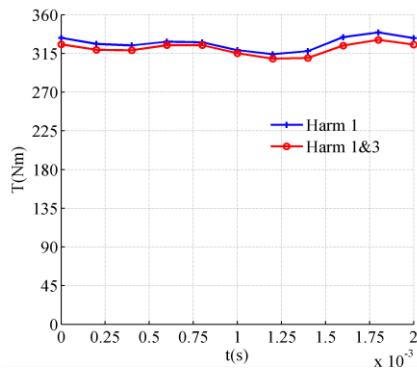
In this paper the previous property is used to reduce the current peak, in order to supply the machine with cheaper inverter or to protect the electronic components. It can be proved that adding a third harmonic current component to the first one can decrease the peak value of this current. A maximum drop in this value (13.4%) is obtained when the added third harmonic component is 16.4% of the first one.

Fig. 15 shows two generated torques in this 5-phase machine with  $h = 12 \text{ mm}$ , the first one is produced by the main current harmonic, the other is the result after adding the third harmonic.

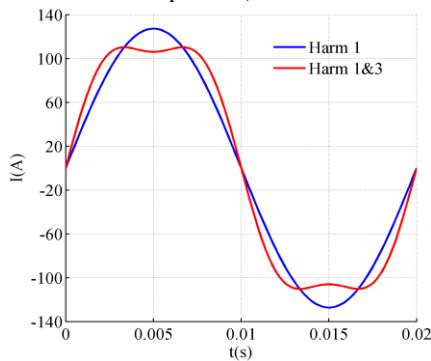
It can be noted that, according to theory of multiphase machine, the third harmonic current has no effect on the torque pulsations for this configuration (since the secondary machine is inactive). In the same time it helps to reduce the current peak by 13.4%. However, this technic leads to 2.7% more Joule losses in the windings. This kind of injection could be used, during transient states (as acceleration), to maximize the use of current rating of the voltage source inverter transistors.

### 3.3 The Cogging Torque

The cogging torque sensibility to  $h$  is also studied for this 5-phase machine using the same methodology consisting in a coupling between an optimization program in matlab and the FEM “femm”. The result shows that straight-shape magnets configuration ( $h = 4.16$  mm) has the lowest cogging torque. Since 8 slots (40 slots instead of 48) are deleted to adapt the stator to 5-phase winding, the cogging torque of this 5-phase machine is higher comparing with the original PRIUS. However, the level cogging torque is much less important than pulsation due to interaction between harmonic of EMF and current. Fig. 16 shows the cogging torque and its RMS value for different  $h$ .



(a) 5-phase machine torque before and after adding the current 3rd harmonic component (16.4% of fundamental)



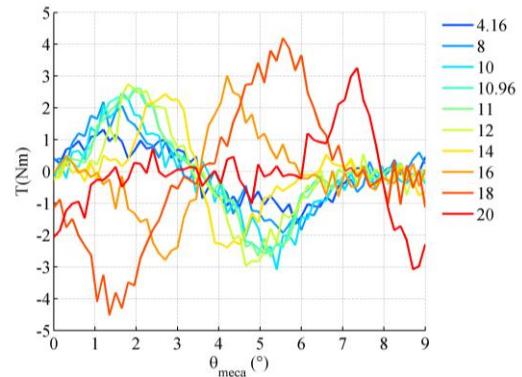
(b) phase current before and after adding the 3rd harmonic component (16.4% of fundamental)

**Fig. 15** Machine torque with lower current peak ( $h = 12$ ).

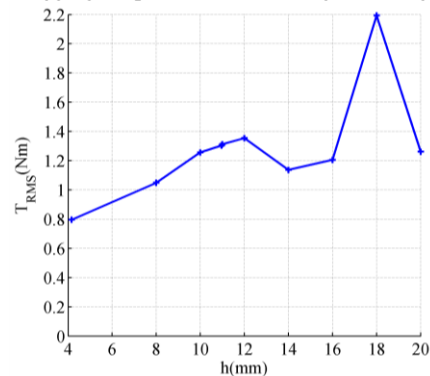
### 3.4 Torque Ripple

Lower pulsating torque is one of the interesting advantages of multi-phase machines [11], owing to the fact that the harmonics which interact to disturb the torque have higher ranks. For example in 5-phase

machines the first disturbing harmonic for main fictitious machine is the 9th instead of the 5th in 3-phase classic machines [10]



(a) Cogging torque for different magnet configurations



(b) RMS value of cogging torque for different magnet configurations

**Fig. 16** Cogging torque for 5-phase PRIUS type machine.

Fig. 17 shows the curves of relative amplitude of torque oscillation, where each curve presents the relative torque oscillation of one configuration ( $h$ ) according to electrical angle  $\psi_e$ , while the machine is supplied with 5 sinusoidal shifted currents (127 A).

After observing the curves until  $\psi_e = -60^\circ$ , it can be found that the configurations with  $4.16 < h < 12$  have the lowest relative oscillation in torque (less than 10%). To analyze this result the EMF frequency spectrums presented in Fig. 14 is studied, it can be seen that the 9th harmonic is almost null in the configurations correspond to lower torque ripples ( $4.16 < h < 12$ ), which proves the role of this harmonic in torque ripples. Besides, the results confirms that third, fifth and seven harmonics, which are much more important than with the 3-phase configuration, have no impact of torque pulsation when sinusoidal currents are imposed.

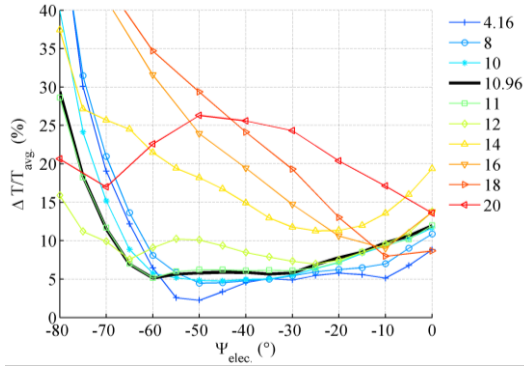


Fig. 17 Torque ripple in 5-phase PRIUS type machine ( $I_p = 127$  A).

In order to compare torque ripple for different configurations, the average value of torque relative oscillation is calculated along the flux weakening region  $\psi_e \in [-80^\circ, -45^\circ]$ . Fig. 18 presents this average according to  $h$ , where it can be noted that the structure with  $h = 10.96$  mm (PRIUS structure) has also the lowest average of torque relative oscillation (about 8%) all over the flux weakening region. To conclude, despite the fact that a simple winding structure is applied in this 5 phase machine (only one slot per pole and per phase), it generates much less torque ripple through the whole flux weakening region and for all magnet configurations.

### 3.5 Flux Weakening Region

As in the last paragraph,  $L_d$ ,  $L_q$  are calculated for the main fictitious machine using FEM “femm”, and in order to consider iron saturation this calculation is done for three different load currents (amplitude 127 A, 99 A, 71 A). Figs. 19a and 19b presents the calculated values of  $L_d$ ,  $L_q$  according to the magnet open angle. The value ( $L_q - L_d$ ) which indicates the added reluctance torque is also represented in Fig. 19c.

In order to study the flux weakening region of the 5-phase machine, the same limits as in original PRIUS machine are considered, 500 V Dc Bus, and maximum current amplitude of 127 A (keeping the same linear current density as for 3-phase machine with 212 A). Using the same flux weakening strategy in the last paragraph, and considering last limits, the curves torque-speed, and power-speed of the machine are

drawn. Fig. 20 shows the curves which present the torque-speed, and power-speed characteristic of the machine for 5 magnet configurations (5 values of  $h$ ).

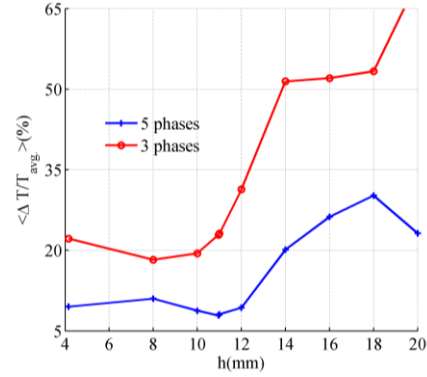


Fig. 18 The average of relative torque ripples over the flux weakening region.

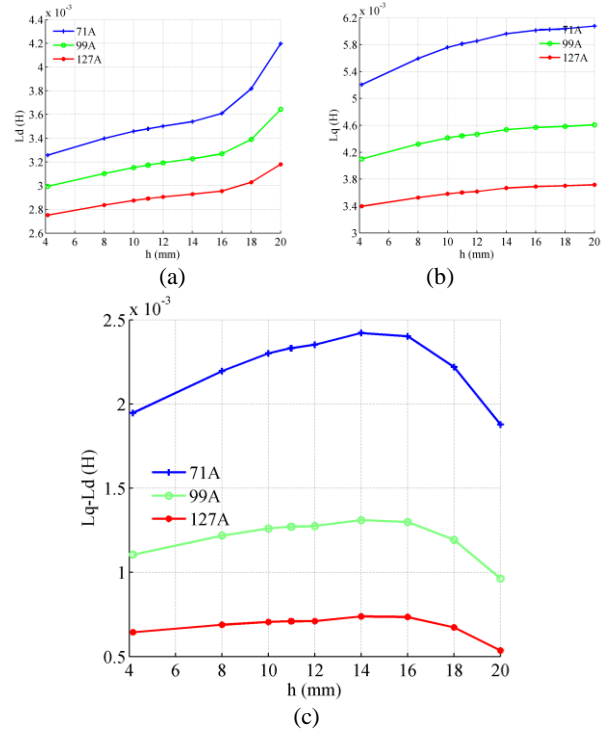


Fig. 19 (a)  $L_d$ , (b)  $L_q$  and (c)  $L_q - L_d$  calculated for 5-phase PRIUS type machine.

As in 3-phase machine it can be noted that, straight-shape magnet configuration ( $h = 4.16$  mm) has the best characteristics torque-speed along the flux weakening region, while the configuration with  $h = 14$  mm seems to produce the maximum torque at basic speed.

Fig. 21 shows the torque/power-speed, characteristics of the machine for the same five values

**Influence of Rotor Structure and Number of Phases on Torque and Flux Weakening Characteristics of V-shape Interior PM Electrical Machine**

of  $h$  but with lower maximum current of 99 A. Here the reluctance effect is clearer, where the configurations generate different torques at basic speed. The structure with  $h = 14$  mm is the best choice at low speed application (more generated torque), while the straight-shape magnet structure stays the best choice for higher speeds along the flux weakening region.

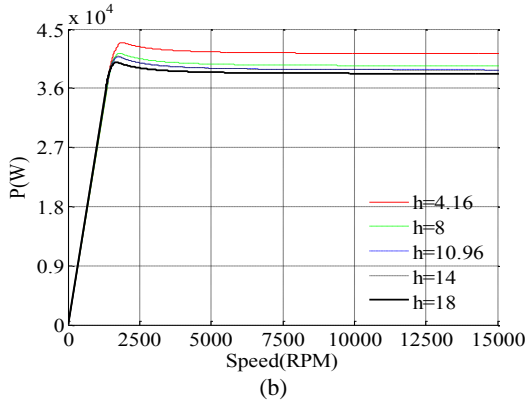
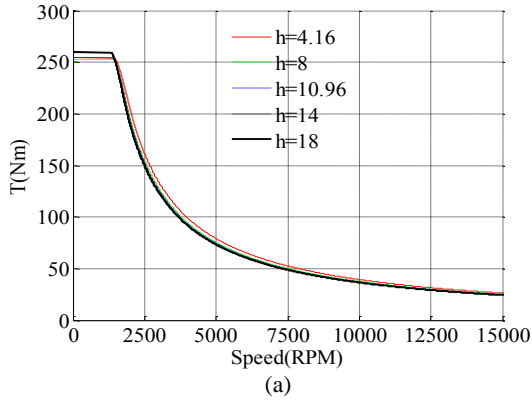


**Fig. 20 (a) Torque-speed, (b) Power-Speed characteristics for the 5-phase PRIUS type machine for  $I_p = 127A$**

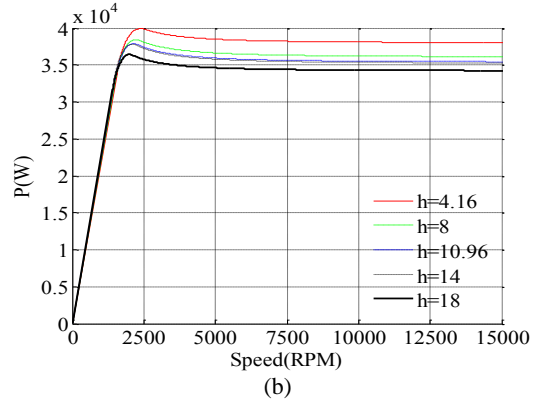
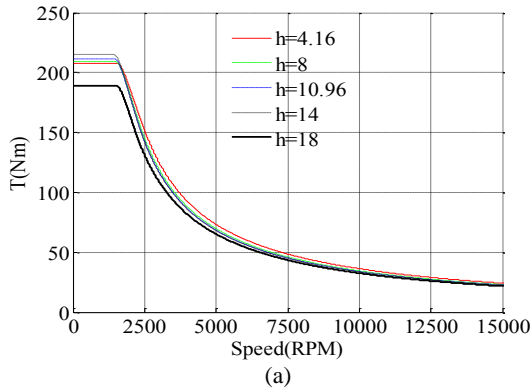


**Fig. 21 (a) Torque-speed; (b) power-speed characteristics for the 5-phase PRIUS type machine for  $I_p = 99 A$ .**

**4. Conclusions**

This paper studies the effects of magnet pole open angle ( $h$ ) on torque and flux weakening region of V-shape magnets PRIUS type machine. Moreover similar study is done for a 5-phase machine which has the same type and dimensions of PRIUS. It shows interest of the modification of the number of phases for the drive.

3-phase PRIUS machine structure with  $h = 10.96$  mm produces the highest average total torque, due to its high reluctant torque which makes 39% of total torque.

Also 3-phase PRIUS structure appears to have very low cogging torque even if the lowest cogging torque is obtained with  $h = 11.5$  mm. On the other hand Torque ripples increase notably with magnet open angle, and the structure with  $h = 8$  mm appears to have the minimum torque ripples all over the flux weakening region (19%) even if 3-phase PRIUS configuration is not so far (22%).

The inductance values  $L_d$ ,  $L_q$  vary also with the pole angle leading to different flux weakening regions, and this study shows that the structure with straight-shape magnets keeps the highest power through the flux weakening region, while PRIUS and the structure with  $h = 14$  mm produce the highest torque at basic speed (before flux weakening).

The modified machine with five phases and 40 slots produces the same average torque as in three phases

case, beside that the 5-phase machine with PRIUS rotor structure ( $h = 10.96$  mm) still offers one of the highest average torques.

Whereas the lower torque ripples is the most obvious advantage of this 5-phase machine, and PRIUS rotor structure with  $h = 10.96$  mm has the lowest average torque ripples all over the flux weakening region (8%) in comparison with 19% in 3-phase configuration.

The additional degree of freedom offered by the 5-phase structure is also used to generate the same torque but with 13.4% lower current peak.

For the flux weakening the conclusion are the same as for 3-phase configuration. In future works, impact of concentrated windings allowing low torque ripples could also be investigated with multiphase configurations.

### **Acknowledgments**

This work was supported by ADEME of France for MHYGALE project

### **References**

- [1] L. Guo, L. Parsa, Effects of magnet shape on torque characteristics of interior permanent magnet machines, in: Electric Ship Technologies Symposium, Baltimore, Maryland USA, Apr. 20-22, 2009, pp. 93-97.
- [2] J.S. Hsu, C.W. Aψers, C.L. Coomer, Report on TOYOTA/PRIUS motor design and manufacturing assessment [Online], OAK Ridge National Laboratory, 2004, www.ornl.gov.
- [3] E. Levi, Multiphase electric machines for variable-speed applications, IEEE Transactions on Industrial Electronics 55 (5) (2008) 1893-1909.
- [4] M. Olszewski, Evaluation of 2004 TOYOTA PRIUS hybrid electric drive system [Online], OAK Ridge National Laboratory, 2006, www.ornl.gov.
- [5] G. Cvetkovski, L. Petkavska, Dynamic simulation of PM disc motor using MATLAB/Simulink coupled with finite element method, in: 13th European Conference on Power Electronics and Applications, Barcelona, Spain, Sept. 8-10, 2009, pp. 1-10.
- [6] M. Kamiya, Development of traction drive motors for the toyota hybrid system, IEEJ Transactions on Industry Applications 126 (4) (2006) 473-479.
- [7] J.R. Figueroa Barnier, "Wide speed range drive modeling for design purposes", PhD thesis, University of Laval Quebec, 2008.
- [8] D. Evans, Z. Azar, L.J. Wu, Z.Q. Zhu, Comparison of optimal design and performance of PM machines having non-overlapping windings and different rotor topologies, in: 5th IET International Conference on Power Electronics, Machines and Drives (PEMD 2010), Brighton, UK, Apr. 19-21, 2010, pp. 1-7.
- [9] Z. Azar, L.J. Wu, D. Evans, Z.Q. Zhu, Influence of rotor configuration on iron and magnet losses of fractional-slot IPM machines, in: 5th IET International Conference on Power Electronics, Machines and Drives (PEMD 2010), Brighton, UK, Apr. 19-21, 2010, pp. 1-6.
- [10] F. Scuiller, J.F. Charpentier, E. Semail, S. Clénet, Comparison of two 5-phase permanent magnet machine winding configurations. application on naval propulsion specifications, in: IEEE International Electric Machines & Drives Conference, Antalya, Turkey, May 3-5, 2007, Vol. 1, pp. 34-39.
- [11] F. Locment, E. Semail, F. Piriou, Design and study of a multiphase axial-flux machine, IEEE Transactions on Magnetics 42 (4) (2006), 1427-1430.